

Improving the error performance of offset pulse position modulation using Reed–Solomon error correction code and low-density parity

Ahmed Hasan Salman¹, Basman Monther Al-Nedawe², Mohamed Ibrahim Shuja'a¹

¹Department of Computer Technology Engineering, Electrical Engineering Technical College, Middle Technical University, Baghdad, Iraq

²Department of Computer Technology Engineering, Technical Institute of Baquba, Middle Technical University, Diyala, Iraq

Article Info

Article history:

Received Jan 31, 2022

Revised Jun 11, 2022

Accepted Jun 21, 2022

Keywords:

Forward error correction
Low density parity check code
Offset pulse position modulation
Reed–Solomon code
Transmission efficiency

ABSTRACT

An innovative performance study of an offset pulse-position modulation (OPPM) scheme is presented in this work with Reed–Solomon (RS) and low-density parity-checking (LDPC). The main aim is to resolve the errors of OPPM three using an RS or LDPC as a sporadic set of forward error correction (FEC). In this regard, the separate FEC has been utilized with coding that is based on multi-level, and waveform shaping based on the trellis. To systematically conduct this research, the greatest transmission efficiency that associated with the optimum RS code rates at different fiber normalization bandwidths is evaluated. Furthermore, the transmission efficiencies, channel extension, as well as the required number of photons per pulse of OPPM before and after the integration with RS or LDPC are compared. The results indicate an enhancement of mitigating the system's bit error rate and delivering more error-free data to the receiver in the occasion of applying the optimal settings of the RS or LDPC.

This is an open access article under the [CC BY-SA](https://creativecommons.org/licenses/by-sa/4.0/) license.



Corresponding Author:

Ahmed Hasan Salman

Department of Computer Technology Engineering, Electrical Engineering Technical College, Middle Technical University

Baghdad, Iraq

Email: bbc0042@mtu.edu.iq

1. INTRODUCTION

Modulation and coding are processes carried out at the transmitter to ensure that information is sent efficiently and reliably. Two waveforms are used in modulation, a message and a carrier, the former represents the information signal, called the modulation signal, while the latter transfers the information and is specific to each application. A modulator changes the carrier wave systematically based on the change within the information signal [1]. We normally need that modulation to be reversible so that the message can be recovered using the appropriate demodulation process. A part of an analog modulating signal and the modulated waveform formed by changing the amplitude of a sinusoidal carrier wave that is called amplitude modulation (AM) which is probably acquainted with radio broadcasts and other uses [2]. Frequency modulation (FM) or phase modulation can also be used to imprint a message on a sinusoidal carrier. Continuous-wave (CW) modulation is the umbrella term for all sinusoidal carrier modulation schemes. The carrier frequency of most long-distance transmission systems is significantly higher than the modulating signal's highest frequency component [3]. This can be attributed to a low mark-to-space ratio. Because it does not contain a lot of markings, digital pulse position modulation (PPM) is said to be excellent at encoding massive data words [4]. Dicode pulse position modulation (DiPPM) is a straightforward method when

considering the practical implementation and coding scheme. When there is no alteration in the pulse code modulation (PCM) signal, there will be a zero pulse. In which, a logic zero occurs and drops from logic one, symbolized by (-V), while coded as (+V) counter-wise.

2. OFFSET PULSE POSITION MODULATION

Offset pulse position modulation (OPPM) has been proposed as a new sort of digital pulse position modulation (DPPM), which can be a preference in optical and free space communication. The OPPM rate is one-half the PPM, however, giving rise to the sensitivity when operating with low bandwidth [5]. Meaning, OPPM rectifies the PPM if considering bandwidth extension. Interestingly, the OPPM improves the sensitivity by more than 3.1 dB over digital PPM, with competent sensitivity if compared to multiple PPM. The procedure of error correction can be identified within a set of sequences. The first sequence is applied when all codeword locations have reset to zero. In the second sequence, the least significant bit (LSB) is discarded in favor of the first sequence. By moving one digit from the least significant towards the most significant, the next code words in the sequence will be produced [6]. Ahfayd *et al.* [7] studied the spectrum properties of OPPM, MPPM, and truncated PPM. This in turn has concluded that the OPPM can produce distinct lines compared to DPPM. However, DPPM has a strong element frame of recurrence rate compared to OPPM. The OPPM technique converts PCM three-bit codewords to four-bit codewords. On the other hand, DPPM has a line rate of 2^m , where m percent of the m-bits is the signal bits in the fundamental PCM rate. m can also be used to illustrate how to convert 3 bits of PCM into OPPM and DPPM codewords Table 1. For instance, the method is comparable to that of DPPM at 100 PCM. However, no pulse is broadcast for 000 PCM when OPPM is of a differential. The most significant bit (MSB) has stripped the PCM term and owns 2^{m-1} delay time slots by the decoder and OPPM coder.

Table 1. PCM to OPPM and DPPM transformation

PCM (Data Word)	OPPM Code Word	DPPM Code Word
000	0 000	0000 0001
001	0 001	0000 0010
010	0 010	0000 0100
011	0 100	0000 1000
100	1 000	0001 0000
101	1 001	0010 0000
110	1 010	0100 0000
111	1 100	1000 0000

For the first time, PPM was successfully implemented on a visible light communication (VLC) system with a 'warm' 30W LED, reaching a data throughput of 11 Mbps and having zero errors in transmission over a 1 m space that is free [8]. OPPM error causes have been addressed by Wang *et al.* [9] using the automatic repeat request (ARQ) method. They demonstrated that OPPM has built-in error-checking capabilities, hence, the performance regarding the frame error rate of OPPM is increased by using ARQ [10].

2.1. OPPM error source

OPPM, like digital PPM, there are three different types of detecting failures: incorrect slot, erase, and false alarm [11]. When a pulse rising edge's noise causes it to appear as adjacent time slots, this is known as a wrong-slot error. The probability of a faulty slot mistake is computed in the following manner.

$$P_{es} = 0.5 \operatorname{erfc} \left(\frac{Q_{es}}{\sqrt{2}} \right) \quad (1)$$

$$Q_{es} = \frac{[T_s \operatorname{slope}(t_d)]}{\left[2 \sqrt{n_o^2} \right]} \quad (2)$$

where T_s is the slot time, t_d is the pulse that was slop received at the moment of decision, and n_o^2 is the noise with a mean square delivered detectors at the upper limit. The pulse time slot whose width T_s , is detected to decrease such error, when the pulse's edge travels $T_s/2$, an error is generated [12].

Erasure errors occur when noise levels are high enough to cause the peaked voltage applied to the signal below the cut-off point, as a consequence of losing a pulse. The likelihood of erasure errors is given by (3).

$$P_{er} = 0.5 \operatorname{erfc} \left(\frac{Q_{er}}{\sqrt{2}} \right) \quad (3)$$

T_s/R denotes the amount of noise that is unrelated bit per time frame. τ_R denotes the point in time when auto correlation has shrunk considerably, and Q_t denotes the time at which the auto correlation has become small.

$$Q_s = \frac{(V_{pk} - v_d)}{2\sqrt{n_0^2}} \quad (4)$$

v_{pk} describes the transmitter voltage level of specific time slot, while v_d denotes the decision voltage.

There is noise at this voltage. If there is no pulse, a threshold crossover may occur, resulting in false alarms. Due to the existence of inter-symbol interference, there may be a signal voltage within slots and around the pulse [13].

$$P_{s=\frac{TS}{\tau R}} = 0.5 \operatorname{erfc} \left(\frac{Q_s}{\sqrt{2}} \right) \quad (5)$$

Per time slot, the number of uncorrelated noise samples is represented by the ratio $T_s/\tau R$, where τR is the moment when the time series produces the minimal value.

$$Q_s = \frac{(v_d - v_{isi})}{\sqrt{n_0^2}} \quad (6)$$

The signal voltage level at a specific time slot is represented by v_{isi} , which is dependent on the fault occurrences.

3. ERROR CORRECTION CODE

3.1. Reed–Solomon error correction

Errors can occur during transmission and storage for a variety of reasons as shown in Figure 1. Reed–Solomon (RS) codes are well-known codes for error correction and are used in different applications and communications networks [14]. The RS encoder augments a chunk of digital information with extra "duplicate" bits. The RS decoder can examine every block to rectify and recover the beginning data [15]. The characteristics RS code control the type and number of retrievable errors. Bose–Chaudhuri–Hocquenghem (BCH) codes are a subclass of RS codes, which are blocks that are linear digits. With m -bit symbols, RS code can be denoted with RS (n, k) [16]. RS is represented in this study to recover the error causes that plague the OPPM. P_E is specifically used to critically represent the symbol-error likelihood encoded by RS as illustrated in (7).

$$P_E = \frac{1}{2^{m-1}} \sum_{j=t+1}^{2^{m-1}} j \binom{2^{m-1}}{j} p^j (1-p)^{2^{m-1}-j} \quad (7)$$

The code's ability to rectify symbol errors is t , and each signal is formed composed of m bits. The likelihood of a decoded symbol outage is proportional to the probability of a binary mistake [17].

$$P_{eb} = \frac{2^{m-1}}{2^{m-1}} \quad (8)$$

The scheme has associated characters like n and k , which can be written as RS utilizes m -bit symbols in his coding.

$$0 < k < 2^M + 2 \quad (9)$$

where k denotes the number of characters in the information that would be decoded throughout the data transmission process using RS codes. n_{RS} denotes the overall sum of characters that are used in the codes contained in the block that holds the codes. It is feasible to create the greatest code essential with the shortest distance (d_{\min}) covered by RS. RS codes can fix t or less types of transmission stream problems as demonstrated in (10) [18].

$$t = \left\lfloor \left(\frac{d_{\min} - 1}{2} \right) \right\rfloor = \left\lfloor \left(\frac{n - k}{2} \right) \right\rfloor \quad (10)$$

Code rate equation can determine by (11).

$$r = \frac{2^{m-1} - 2t}{2^{m-1}} \quad (11)$$



Figure 1. RS coding scheme [19]

3.2. Low-density parity-check

Theoretically, it can be stated that the linearly fault correcting code (LFCC) is a low-density parity check (LDPC) that is used to deliver information through a chaotic communication system [20]. The bipartite graph's subclass is used to create LDPC. LDPC codes allow the noise limit for a symmetrical memoryless channel to be set very close to the theoretical maximum. The noisy thresholds provide an upper limit for channel noise with maintaining the risk of data loss to the lowest possible level. In this regard, the iterative propagation methods can be used to decode LDPC codes in a way to characterize the block length [21]. LDPC codes are widely employed in several applications which necessitate accuracy to fix the corrupting noise. LDPC is an effective and highly economical transmission of information throughout a network with a restricted return channel. Figure 2 shows the graphical representation of LDPC codes with the device variable's temporal variation ($v_o(t)$). Specifically, this is the Tanner bipartite graph that provides an excellent graphical depiction of LDPC codes. The description of the decoding procedure is clearly shown in Figure 2 where two disjoint groups of nodes are identified [22].

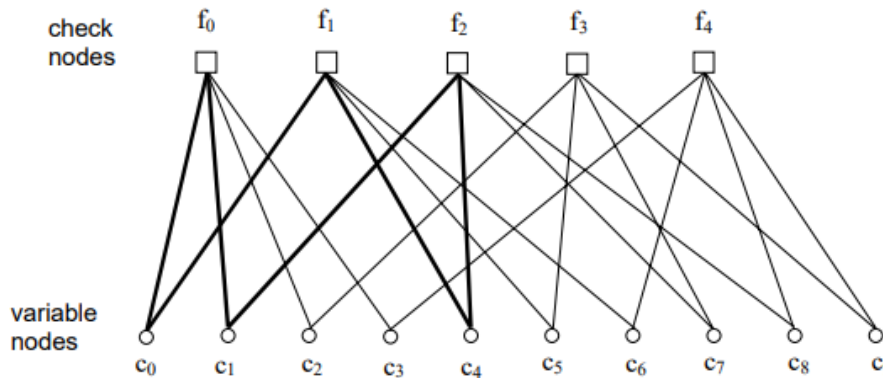


Figure 2. Tanner graph for LDPC codes

Variable nodes (VND) and check nodes (CND) are common types of nodes. VNDs are the nodes that represent the code bits. As a result, one VND represents each of the n columns of the H matrix. CNDs are the nodes that represent the code limitations. As a result, each of the m rows of the H matrix is represented by a single CND [23].

If $H_{i,j}=1$, each "variable node" V_i will link to a "check node" C_j , as depicted in the following matrix:

$$H = \begin{pmatrix} 0 & 1 & 0 & 1 & 1 & 0 & 0 \\ 1 & 1 & 1 & 0 & 0 & 1 & 0 \\ 0 & 0 & 0 & 0 & 0 & 0 & 1 \\ 1 & 0 & 1 & 1 & 0 & 1 & 0 \end{pmatrix}$$

There are two types of LDPC codes: regular and irregular. Each column of H in the normal LDPC codes has precisely V ones, and each row of H contains exactly C ones [24]. As a result, a normal LDPC code is defined just by the values of V and C [25]. The H-Matrix is used to encode the LDPC codes. This H-Matrix may be created in two ways for a normal LDPC code Gallager's method and MacKay and Neal method [26].

4. THE PROPOSED MODEL

The model is based on the paradigm suggested by Sibley [1]. The model has been coded in Mathcad and simulated. The receiver's architecture is shown in Figure 3. In the simulation process, a limited bandwidth ω_c based optical receiver has been used. In addition, white noise has been injected at the output. Mathcad filter is presented as a primary filter because of the white noise existence. POF, which is a graded index, has been used as a channel to transmit the PPM signal. Moreover, the threshold detector's signal can be given (12).

$$v_o(t) = b\eta qR_T \frac{\omega_c}{2} \exp(\alpha^2 \omega^2) \times \exp(-\omega_c t) \operatorname{erfc}[\alpha \omega_c - (\frac{t}{2\alpha})] \tag{12}$$

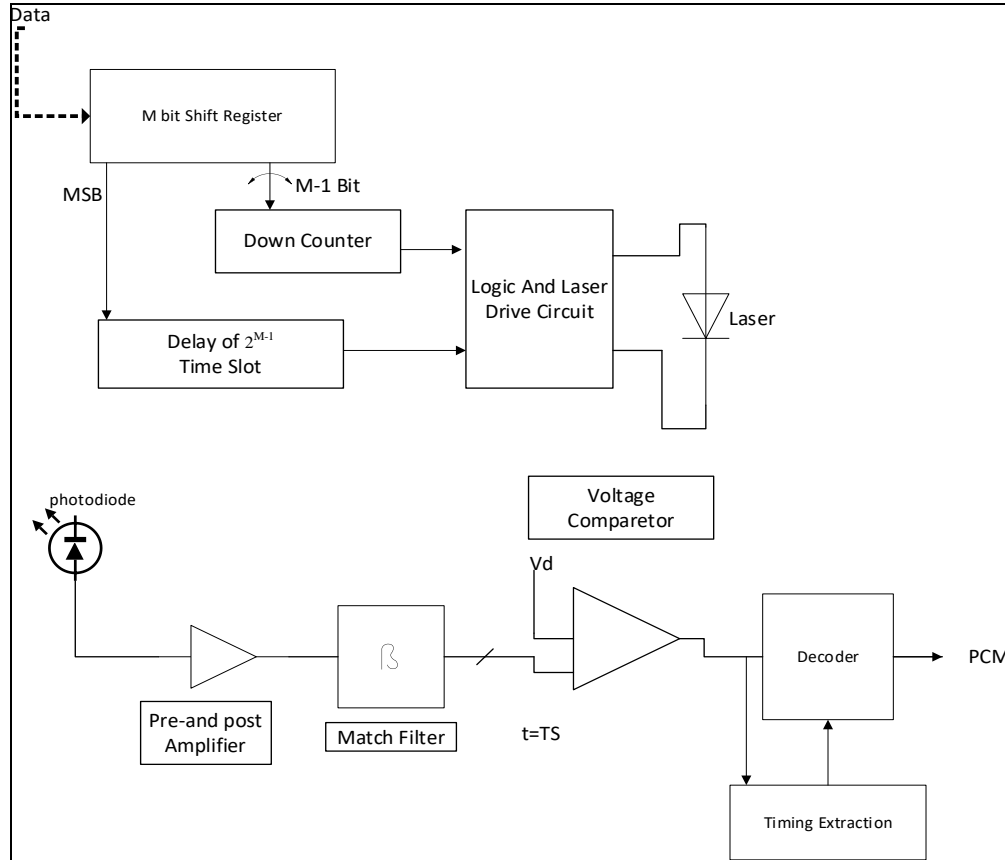


Figure 3. System for OPPM coding and transmission

Photons number at each pulse has been denoted as b , and η represents the detector's quantum efficiency. Moreover, the electronic charge is noted as q , the center-band transimpedance is symbolized as R_T , and the Gaussian pulse variance is α .

$$\alpha = \frac{0.1874T_b}{f_n} \tag{13}$$

Moreover, the bit time of PCM is symbolized as T_b , f_n denotes the bandwidth of the fiber that is normalized to data rate of the PCM. The appearing noise on PCM signal can be presented as (14) and (15).

$$\langle n_o^2 \rangle = S_o \frac{\omega_c}{2} R_T^2 \exp(\alpha^2 \omega_c^2) \operatorname{erfc}(\alpha \omega_c) \tag{14}$$

$$v = \frac{v_d}{v_{pk}} \tag{15}$$

where S_o denotes the spectral density of the preamplifier's noise current, that is double-sided. In the simulation process, a PIN photodiode has been utilized while neglecting its shot noise. The time becomes

small that its filter output's auto-correlation function, the time is considered as α , hence $\tau_R = \alpha$. It was denoted that the variable threshold level is v , and given in (20), at which, the isolated pulse's peak voltage is given as v_{pk} . Given the bandwidth of the fiber, the noise and the shape of the pulse are measured, where the maximum of v which results in the least photons number in each pulse, is found for a certain error rate of the PCM (in the simulation, 1 at each 10^9). The PCM system also operated a data-rate equivalent to 1 Gbit/s, 650 nm wavelength, while the quantum efficiency of the photodiode is 100%. The bandwidth of the preamplifier is equivalent to 10 GHz. In addition, the white noise is equal to $50 \times 10^{-24} \text{ A}^2/\text{Hz}$. The operational parameters have been used using a commercial instrument. was used so that $n_{DiPPM} = 10$, which represents the data of the line coded PCM. Results are produced from DiPPM while cooperating without and with RS code [27].

5. RESULTS AND DISCUSSION

This section aims to study the effect of the pulse's photons number while conducting OPPM coding when the central detection method has been utilized at various coding velocities. m values have been selected as 3, 4, and 5, and the photon count is directly measured as 2^m codewords. It is essential to note that when the rate of the RS coding increases, the number of photons will be proportionally increased. This is because of the stable relation between RS coding velocities and the number of data symbols.

5.1. Number of photons versus RS code rate at various code levels

Basically, minimizing the number of photons in a pulse is recommended to create the ideal implication of the RS code rate and accelerated the maximum performance of the device. Figure 4 illustrates the influence of the varying numbers of photons of an OPPM on the RS coding rate at m (code level). Undoubtedly, the fault rate of the system was kept to a minimum during this action. An inverse relationship is illustrated between a number of photons and the number of standardized bandwidths. The maximum normalized bandwidth corroborates the lowest value of a number of photons. In addition, when the RS coding rate rises, a number of photons grows exponentially.

5.2. Transmission efficiency versus RS code rate at various code levels

The coded OPPM's transmission efficiency in counters to RS coding rates normalized bandwidths with numerous fibers is represented in Figure 5. For the broadest possible range of normalized bandwidths, it was indicated in Figure 5, that the best transmission efficiency is about 0.6. Yet, with narrower normalized bandwidth, the highest transmission efficiency was acquired at roughly 0.7 RS coding rate. It was vital that understanding the code rate and transmission effectiveness are exponentially related since the efficacy is effectively zero once the optimal code rate is reached. In other words, as the pace of coding has increased, errors of unrecorded symbols, have increased too. Consequently, the system's effectiveness and ability to transmit symbols that have been rectified are reduced. In this example, both, the rate, and amount of redundancy have exceeded the optimal coding rate. On contrary, increasing the normalized bandwidth of the fiber caused the transmission efficiency to be increased too. Figures 4 and 5 illustrate the critical nature of lowering b via the use of RS codes to maximize the transmission efficiency of OPPM.

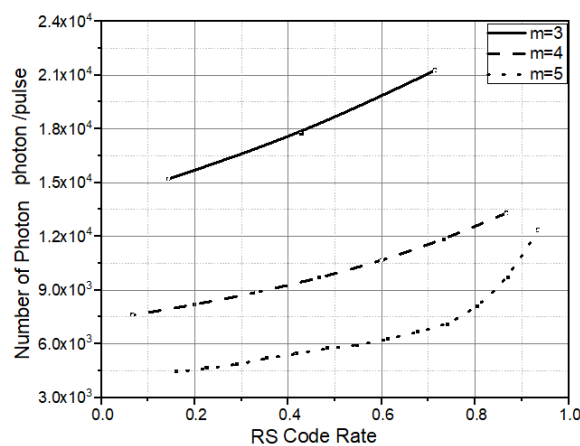


Figure 4. Photons number versus RS code rate at various code levels

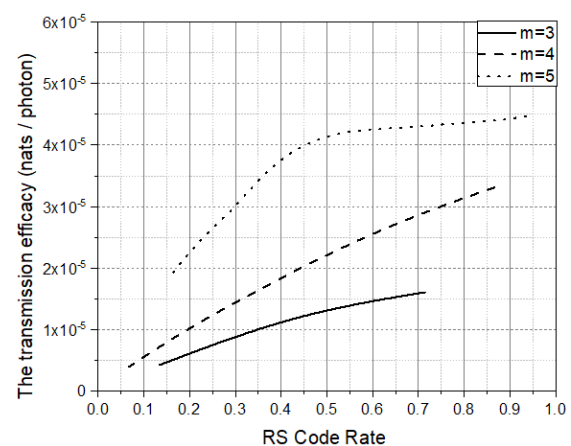


Figure 5. The OPPM transmission efficiency versus RS code rates at different code levels

5.3. Number of photons versus RS code rate at different normalized bandwidths

For many normalized fiber bandwidths (f_n), Figure 6 depicts the evolution of the quantity for the coded OPPM system in pulse's photons against the code rate of the RS. For every given normalized bandwidth, there is a straight positive connection between the RS code rate and b . For a certain bandwidth, the number of photons increases as a result of increasing the RS code rate.

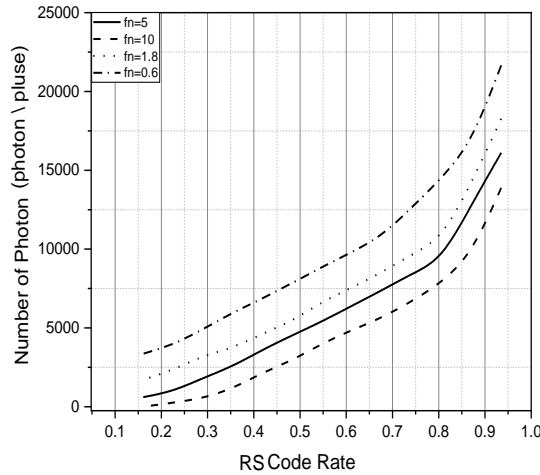


Figure 6. Photons number with the coding rate of the RS at many normalized bandwidths

5.4. The OPPM transmission efficiency versus RS code rate at various normalized bandwidths

The link between the RS code rate (f_n) and the transmission efficiency of the OPPM using the RS code scheme for different normalized bandwidths has been shown in Figure 7 with respect to the OPPM data rate. The usage of an optimal code rate of 0.7 is to improve the total efficiency. For low dispersive channels, the RS coding based coded OPPM achieves the best transmission efficiency based on the following correlation.

$$\alpha = \frac{0.1874 T_b}{f_n} \tag{16}$$

T_b is the PCM bit-time.

$$\rho = \frac{r \ln 4}{b} \tag{17}$$

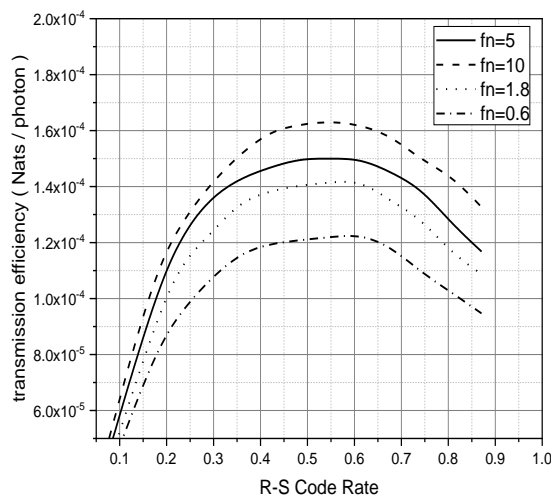


Figure 7. The OPPM transmission efficiency versus RS code rate at various normalized bandwidths

5.5. Comparing the OPPM transmission efficiency employing different error correction codes

Figure 8 demonstrates the transmission efficiency of OPPM, RS, and LDPC codes based on the normalized bandwidth. Clearly, incorporating the LDPC into OPPM has achieved a greater transmission efficiency than RS and OPPM when working. This is owing to the fact that the LDPC code requires more bandwidth as a result of the redundancy symbols.

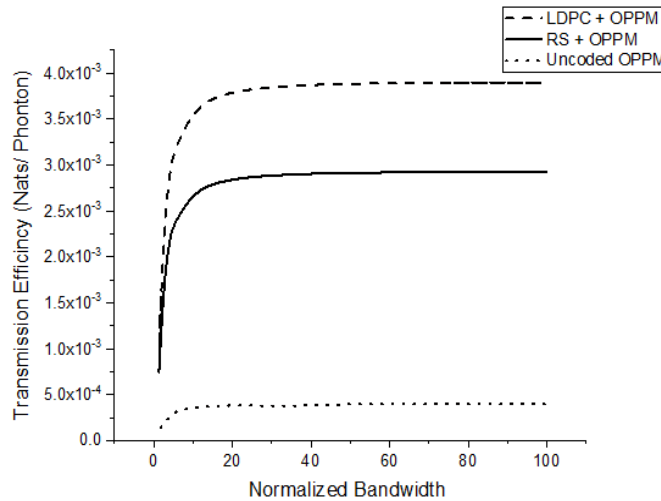


Figure 8. Transmission efficiency at optimum code rate for the OPPM with and without error correction code

5.6. Influence of number of photons for uncoded and coded OPPM on the bit error rate

Figure 9 demonstrates a comparison amongst the LDPC, OPPM, and RS based on the photons' number per pulse against the bit error rate (BER). The primary goal of any communication system is to receive and sent data with the possible lowest mistakes. In this regard, the BER unitless measure should be accounted for by the modulation technology. Simply, reducing BER means a reduction in the number of mistakes that enables the predecessor to deliver more data that is error-free to the receiver.

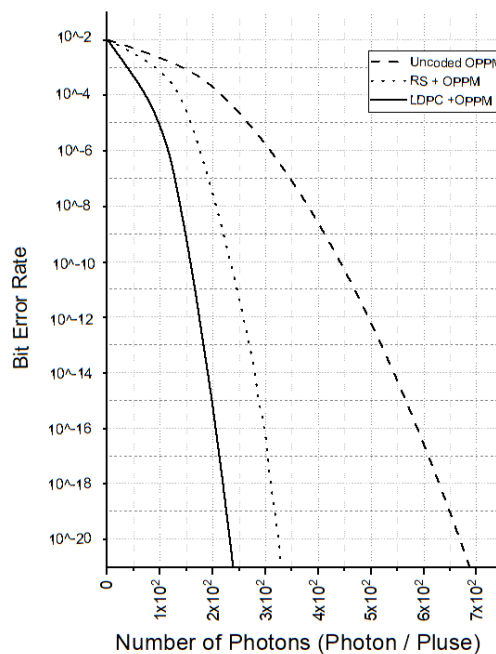


Figure 9. Photons' number for RS, LDPC and OPPM against different bit error rate

6. CONCLUSION

With the use of OPPM, this article studied the transmission efficiency, and the number of photons needed per one pulse for the RS codes or LDPC simulation. It has been concluded that the programmed mechanism of the OPPM overcomes the systems that are uncoded. The received signal has been measured by enhanced central detection techniques to accomplish the study's primary objective. It is therefore fair to claim that the fulfillment of a high transmission efficiency of OPPM can be attained by lowering the number of photons per pulse sent through RS codes or LDPC. Also, increasing the LDPC codeword and RS would positively increase the performance of the machine. The ideal LDPC coding rates with respect to the low and high dispersive fiber channels, which have demanded the highest transmission efficacy addressed in this research resulted in the highest transmission efficiency. We can use this work design in telecom transmission and fiber systems.




REFERENCES

- [1] M. J. N. Sibley, "Analysis of offset pulse position modulation – a novel reduced bandwidth coding scheme," *IET Optoelectron.*, vol. 5, no. 4, pp. 144–150, Aug. 2011, doi: 10.1049/iet-opt.2010.0013.
- [2] S. S. Hreshee, "Automatic recognition of the digital modulation types using the artificial neural networks," *International Journal of Electrical and Computer Engineering (IJECE)*, vol. 10, no. 6, pp. 5871–5882, Dec. 2020, doi: 10.11591/ijece.v10i6.pp5871-5882.
- [3] I. Garrett, "Digital pulse-position modulation over dispersive optical fiber channels," *International Workshop on Digital Communications*, Tirrenia, Italy, Aug. 1983, doi: 10.1109/TCOM.1983.1095842.
- [4] I. Garrett, "Pulse-position modulation for transmission over optical fibers with direct or heterodyne detection," *IEEE Transactions on Communications*, vol. 31, no. 4, pp. 518–527, Apr. 1983, doi: 10.1109/TCOM.1983.1095842.
- [5] I. Ray, "Analysis of offset pulse position modulation," Ph.D. dissertation, Department of Engineering and Technology, University of Huddersfield, 2015.
- [6] I. Ray, M. J. N. Sibley, and P. J. Mather, "Spectral characterisation of offset pulse position modulation," *IET Optoelectron.*, vol. 9, no. 6, pp. 300–306, Dec. 2015, doi: 10.1049/iet-opt.2014.0035.
- [7] M. H. Ahfayd, M. J. N. Sibley, P. J. Mather, and P. I. Lazaridis, "Visible light communication based on offset pulse position modulation (Offset-PPM) using high power LED," in *2017 XXXIIInd General Assembly and Scientific Symposium of the International Union of Radio Science (URSI GASS)*, Aug. 2017, pp. 1–4, doi: 10.23919/URSIGASS.2017.8105136.
- [8] A. Hamza and T. Tripp, "Optical wireless communication for the internet of things: Advances, challenges, and opportunities," *Preprint*, pp. 1–28, 2020, doi: 10.36227/techrxiv.12659789.
- [9] H. Wang, G. Cheng, X. Sun, and T. Zhang, "Performance analysis of dicode pulse position modulation for optical wireless communications," in *2007 International Conference on Wireless Communications, Networking and Mobile Computing*, Sep. 2007, pp. 3027–3030, doi: 10.1109/WICOM.2007.752.
- [10] S. Lin and D. Costello, *Error control coding fundamentals and application*. London: Prentice-Hall, Inc., 1983.
- [11] R. Charitopoulos and M. Sibley, "Experimental coder/decoder of dicode pulse position modulation," in *Proceedings of Computing and Engineering Annual Researchers' Conference 2009: CEARC'09*, 2009, pp. 124–129.
- [12] M. J. N. Sibley, "Dicode pulse-position modulation: a novel coding scheme for optical-fibre communications," *IEE Proceedings - Optoelectron.*, vol. 150, no. 2, pp. 125–131, Apr. 2003, doi: 10.1049/ip-opt:20030386.
- [13] M. Sibley, "Performance analysis of a dicode PPM system, operating over plastic optical fibre, using maximum likelihood sequence detection," *IEE Proc. - Optoelectron.*, vol. 152, no. 6, pp. 337–343, Dec. 2005, doi: 10.1049/ip-opt:20050009.
- [14] H. Joki, J. Paavola, and V. Ipatov, "Analysis of reed-solomon coding combined with cyclic redundancy check in DVB-H link layer," in *2005 2nd International Symposium on Wireless Communication Systems*, pp. 313–317, doi: 10.1109/ISWCS.2005.1547711.
- [15] S. Egorov and G. Markarian, "Error correction beyond the conventional error bound for Reed-Solomon codes," *Journal of Electrical Engineering*, vol. 54, no. 11–12, pp. 305–310, 2003.
- [16] F. R. Lone, A. Puri, and S. Kumar, "Performance comparison of reed solomon code and BCH code over rayleigh fading channel," *International Journal of Computer Applications*, vol. 71, no. 20, pp. 23–26, 2013, doi: 10.5120/12603-9397.
- [17] R. A. Cryan and J. M. H. M. O. Elmighani, "Reed-Solomon coded optical PPM employing PIN-FET receivers," in *Proceedings of ICC/SUPERCOMM'94 - 1994 International Conference on Communications*, 1994, pp. 126–130, doi: 10.1109/ICC.1994.369009.
- [18] B. M. Al-Nedawe, "Microelectronic implementation of dicode PPM system employing RS codes," Ph.D. dissertation, University of Huddersfield Repository, 2014.
- [19] Y. Fang, Y. Bu, P. Chen, F. C. M. Lau, and S. Al Otaibi, "Irregular-mapped protograph LDPC-coded modulation: A bandwidth-efficient solution for 6G-enabled mobile networks," *IEEE Transactions on Intelligent Transportation Systems*, pp. 1–14, 2021, doi: 10.1109/TITS.2021.3122994.
- [20] B. R. Kadhim and F. Korkmaz, "Reducing LDPC decoder complexity by using fpga based on min sum algorithm," *Kufa J. Eng.*, vol. 13, no. 1, pp. 82–101, Jan. 2022, doi: 10.30572/2018/kje/130105.
- [21] F. S. Hasan, M. F. Mosleh, and A. H. Abdulhameed, "FPGA implementation of LDPC soft-decision decoders based DCSK for spread spectrum applications," *International Journal of Electrical and Computer Engineering (IJECE)*, vol. 11, no. 6, pp. 4794–4809, Dec. 2021, doi: 10.11591/ijece.v11i6.pp4794-4809.
- [22] R. Yazdani and M. Ardakani, "An efficient analysis of finite-length LDPC codes," in *2007 IEEE International Conference on Communications*, Jun. 2007, pp. 677–682, doi: 10.1109/ICC.2007.116.
- [23] Junan Zhang and A. Orbitsky, "Finite-length analysis of LDPC codes with large left degrees," in *Proceedings IEEE International Symposium on Information Theory*, Jun. 2007, p. 3, doi: 10.1109/ISIT.2002.1023275.
- [24] L. Dai, Y. Fang, Z. Yang, P. Chen, and Y. Li, "Protograph LDPC-coded BICM-ID with irregular CSK mapping in visible light communication systems," *IEEE Transactions on Vehicular Technology*, vol. 70, no. 10, pp. 11033–11038, Oct. 2021, doi: 10.1109/TVT.2021.3106053.
- [25] S. Bhooshan, "Pulse modulation," in *Lecture Notes in Electrical Engineering*, 2022, pp. 355–396, doi: 10.1007/978-981-16-4277-7_8.
- [26] Y. M. Hussein, A. H. Mutlag, and B. M. Al-Nedaw, "Comparisons of soft decision decoding algorithms based LDPC wireless communication system," in *IOP Conference Series: Materials Science and Engineering*, 2021, vol. 1105.




- [27] A. H. Albatoosh, M. I. Shuja'a, and B. M. Al-Nedawe, "Effectiveness Improvement of Offset Pulse Position Modulation System Using Reed-Solomon Codes," in *2022 International Congress on Human-Computer Interaction, Optimization and Robotic Applications (HORA)*, Jun. 2022, pp. 1–5. doi: 10.1109/HORA55278.2022.9800066.

BIOGRAPHIES OF AUTHORS






Ahmed Hasan Salman    was born in Iraq on February 10, 1989. He received his B.Sc. in science physics in 2011 from Basra University also he received his B.Sc. in Computer Engineering Techniques Kunooz University, Basra Iraq, in 2019. he is currently pursuing his M.Sc. program in Computer Technical Engineering with an emphasis on communication systems. He can be contacted at bbc0042@mtu.edu.iq.



Basman Monther Al-Nedawe    is a lecturer at the Technical Institute of Baqubah at the Middle Technical University, Baghdad where he has been a faculty member since 2004. He is the head of the Technical Computer Department since 2017. He completed his Ph.D. at Huddersfield University, UK, and his undergraduate studies at Technology University (Iraq). His research interests lie in the area of communication systems, ranging from theory to design to implementation. He has collaborated actively with researchers in several other disciplines of electrical engineering, particularly error correction code systems on problems at the hardware/software interface. The author has participated in many national and international scientific conferences, and he supervises an M.Sc. program. Moreover, he has problem-solving skills, developed verbal and written communication skills at university due to many reports and papers, and presentations. He is cooperative and capable of contributing positively while working as a part of a team due to group work at university also he is open-minded to differences of opinion and has negotiation skills. He can be contacted at email: b.al-nedawe@mtu.edu.iq.



Mohamed Ibrahim Shuja'a    is a member of Electrical Engineering College, Middle Technical University Baghdad (MTU). He has more than 15 years of experience in neural network and network systems and in both the industry and academic sectors and has been involved at various levels of VLSI design such as encryption and decryption, head motion detection, analog, and digital circuit design. Currently, he is actively researching new techniques on IOT using DNA and stream cipher to increase the level of encryption. His research interests include raspberry pi and microcontroller, low-power algorithms and architectures design, image and video processing, and network. He can be contacted at drshujaa@mtu.edu.iq.